

**Stretched extra dimensions and bubbles of nothing in a toy model landscape**

I-Sheng Yang\*

*ISCAP and Physics Department, Columbia University, New York, New York, 10027, USA*

(Received 12 January 2010; published 25 June 2010)

Using simple 6D junction conditions, we describe two surprising geometries. First in a case of transitions between  $dS_4 \times S_2$  vacua, the  $S_2$  can be stretched significantly larger than the vacuum values both before and after the transition. The same mechanism can also lead to “bubble of nothing” geometries.

DOI: [10.1103/PhysRevD.81.125020](https://doi.org/10.1103/PhysRevD.81.125020)

PACS numbers: 11.27.+d, 04.40.Nr

**I. INTRODUCTION AND OUTLINE**

The six-dimensional Einstein-Maxwell theory [1,2] provides stable compactifications to  $M_4 \times S_2$ , where  $M_4$  can be de Sitter, anti-de Sitter or Minkowski space. Recently it is recognized as a good toy model to study transitions between different vacua with compactified extra dimensions [3–5], a scenario that arises from the landscape of string theory [6].

One advantage of this model is that we can have a lot of 4D vacuum solutions with similar sizes of  $S_2$ . Therefore, it is natural to assume that  $S_2$  remains in a similar size during vacuum transitions, as we usually do in more detailed models. However, Johnson and Larfors in [7] pointed out a problem of such assumption in a string theory model.

In Sec. II, we will give an intuitive picture explaining why freezing the extra dimensions during vacuum transitions is generally not a good idea. The interpretation is slightly different from [7] but the main idea is the same.

In Sec. III, we go over general equations in the 6D Einstein-Maxwell theory. Here the transitions are approximated as charged branes at the boundary between vacua, and apply Israel junction conditions to solve the spacetime geometry.

In Sec. IV, we study 4D to 4D transitions with the geometric method and the conventional dimensional reduced method side by side. Together they allow us to describe how the extra dimension changes during the transition. Choosing some allowed values of a free parameter ensures that the extra dimensions are stretched during the process.

In Sec. V, we use the same construction for a new 4D to 6D transition. Different from both the compactification [5] and the decompactification [8], our solution does not have 6D asymptotics. It is similar to a bubble of nothing [9] within a 4D vacuum.

Finally, in Sec. VI we summarize and comment on possible future directions. The stretched extra dimensions may change our picture on bubble collisions [4,10], and help to clarify whether in some cases the transition will be forbidden [7]. The bubble of nothing [9] may replace the

decompactification to be the universal instability in models with extra dimensions.

**II. BETTER NOT TO FREEZE THE EXTRA DIMENSIONS**

Figure 1 is a typical effective (Euclidean) potential of a theory with extra dimensions and discrete vacua. It contains the following two traits.

- (i) In the  $\phi$  direction, the potential gradually slopes to zero, which corresponds to decompactifying the extra dimensions. This can be the real part of Kähler moduli for string theory [11].
- (ii) Discrete vacua distribute not only in the above direction, but also in some other directions  $\psi$ . For example the imaginary part of Kähler moduli in [12].

Because the discrete vacua are stabilized by nonperturbative effects, for the value  $\psi$  not supporting any vacuum, the effective potential typically follows the general slope in  $\phi$ .

Now consider two vacua with the same value of  $\phi$ , namely, the same size of extra dimensions. Fixing that size during a transition implies connecting the two vacua by a straight line in Fig. 1. This line certainly does not obey any equation of motion, as it should be swept away by the nonzero slope in the  $\phi$  direction. A more reasonable path

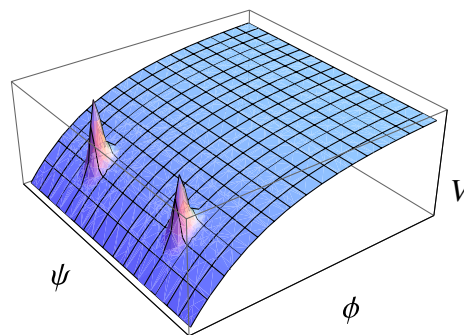


FIG. 1 (color online). An effective Euclidean potential for a theory with extra dimensions and discrete vacua.  $\phi$  is related to the size of extra dimension, so there is a decompactification direction where  $V$  is asymptotically zero. In two different values of  $\psi$  but very similar values of  $\phi$  we have two local maxima—the vacua.

\*isheng.yang@gmail.com

representing the transition would be like a projectile motion—climb the slope in  $\phi$  direction and come back, in the meanwhile move from one vacuum to another. This implies the extra dimension during a transition can be very different from its vacuum value.

Such transition might be very annoying to model, since a generic multidimensional effective potential will not be as simple as Fig. 1 and one can only search for the path numerically. In the following two sections we will show that in the 6D Einstein-Maxwell theory, there is a simple way to monitor transitions with significant changes in the extra dimensions.

### III. 6D SPACETIME WITH VACUUM ENERGY AND FLUX

#### A. Stable solutions

We consider the 6D Einstein-Maxwell theory with positive vacuum energy  $\Lambda_6$  and 4-form fields, as it is appropriate to ensure  $dS_4 \times S_2$  compactifications. For the solutions we will use in this paper, it is most convenient to write down a general metric with  $SO(3, 1) \times SO(3)$  symmetry.

$$ds^2 = d\rho^2 + A^2(\rho)dS_3^2 + B^2(\rho)d\Omega_2^2. \quad (1)$$

The Einstein equations are

$$\begin{aligned} \frac{1}{m_6^4} \left( \Lambda_6 + \frac{Q^2}{4B^4} \right) &= 3 \frac{1 - \dot{A}^2}{A^2} - 6 \frac{\dot{A}\dot{B}}{AB} + \frac{1 - \dot{B}^2}{B^2}, \\ \frac{1}{m_6^4} \left( \Lambda_6 + \frac{Q^2}{4B^4} \right) &= \frac{1 - \dot{A}^2}{A^2} - 2 \frac{\ddot{A}}{A} - 4 \frac{\dot{A}\dot{B}}{AB} + \frac{1 - \dot{B}^2}{B^2} \\ &\quad - 2 \frac{\ddot{B}}{B}, \end{aligned} \quad (2)$$

$$\frac{1}{m_6^4} \left( \Lambda_6 - \frac{Q^2}{4B^4} \right) = 3 \frac{1 - \dot{A}^2}{A^2} - 3 \frac{\ddot{A}}{A} - 3 \frac{\dot{A}\dot{B}}{AB} - \frac{\ddot{B}}{B}.$$

Here  $m_6$  is the 6D Planck mass and  $Q$  is the quantized charge as the field sources, namely, 2-branes. The 6D dS space is a solution with  $Q = 0$ , which corresponds to

$$A(\rho) = L \cos\left(\frac{\rho}{L}\right), \quad (3)$$

$$B(\rho) = L \sin\left(\frac{\rho}{L}\right), \quad (4)$$

where  $0 < \rho < \pi/2$ ,  $10m_6^4 L^{-2} = \Lambda_6$ . Of course we can interchange  $A$  and  $B$ , it is still the same solution.

Nonzero  $Q$  induces “compactified” solutions as

$$A(\rho) = \frac{\sin(H\rho)}{H}, \quad (5)$$

$$B(\rho) = R. \quad (6)$$

Here it is given in the convenient form for dS spaces, but

we can easily take  $H \rightarrow 0$  for Minkowski space and imaginary  $H$  for AdS spaces. Using the Einstein equations, we can relate the size of the compactified dimensions  $R$  and the 4D Hubble constant  $H$  to both  $Q$  and  $\Lambda_6$ .<sup>1</sup>

$$3H^2 + \frac{1}{R^2} = \frac{1}{m_6^4} \left( \Lambda_6 + \frac{Q^2}{4R^4} \right), \quad (7)$$

$$6H^2 = \frac{1}{m_6^4} \left( \Lambda_6 - \frac{Q^2}{4R^4} \right). \quad (8)$$

#### B. Transitions between different solutions

From the geometric point of view, vacuum transitions are related to geometries with solutions of different  $Q$ s patched together. For example, two different solutions separated by a charged 2-brane at  $(\bar{A}, \bar{B})$ . Note that a boundary in 6D is a 5D object, but 2-branes are only 3D objects. We have to sprinkle the branes in two of the dimensions like dust to construct a 5D boundary.<sup>2</sup>

Such patched solutions must obey Israel junction conditions [15] at the boundary. The sprinkled branes are like dilute gas, whose energy is dominated by the rest mass, therefore the pressure is zero.

$$2 \left( \frac{\dot{A}_1 + \dot{A}_2}{\bar{A}} \right) + 2 \left( \frac{\dot{B}_1 + \dot{B}_2}{\bar{B}} \right) = \frac{1}{m_6^4} \left( \frac{\sigma}{4\pi\bar{B}^2} \right), \quad (9)$$

$$3 \left( \frac{\dot{A}_1 + \dot{A}_2}{\bar{A}} \right) + \left( \frac{\dot{B}_1 + \dot{B}_2}{\bar{B}} \right) = 0. \quad (10)$$

It is basically the integrated Einstein equations with a delta-function source.  $\sigma$  is the total tension (energy density in 2D) of the 2-branes we sprinkled on the  $4\pi\bar{B}^2$  sphere. Here the convention is that  $\dot{A}_i > 0$  means  $A_i$  is increasing while moving toward the boundary, and the same for  $B_i$ . Note that for a given fundamental theory  $\sigma$  is proportional to the charge of the brane, but we treat it as a free parameter in order to study vacuum transitions in different fundamental theories.

Note the positivity constraint on the tension,

$$\frac{\sigma}{4\pi\bar{B}^2 m_6^4} = -4 \left( \frac{\dot{A}_1 + \dot{A}_2}{\bar{A}} \right) > 0. \quad (11)$$

<sup>1</sup>Some of the solutions are unstable [13,14], but the solutions we use in Sec. IV are all stable ones.

<sup>2</sup>In realistic situations that such geometry comes from a quantum tunneling, the flux is usually changed by only 1 unit, therefore only involve a single brane as described in [4]. However, a single brane will be a pointlike object on the extradimensional  $S_2$  and ruin the symmetry. Since eventually we care more about the effective 4D picture where the exact location of the brane should not matter, the assumption of sprinkled branes will be sufficient.

Combining Eq. (10) with Eq. (2), we have

$$6 \frac{\dot{A}_1^2 - \dot{A}_2^2}{\bar{A}^2} = \frac{Q_1^2 - Q_2^2}{4m_6^4 \bar{B}^4}. \quad (12)$$

These tell us an important message. For example, when  $Q_1 < Q_2$ , we have  $\dot{A}_1^2 < \dot{A}_2^2$ . So  $\dot{A}_2$  needs to be negative to make the tension positive. More generally, approaching the junction from the side with the larger  $Q$  always looks like approaching a small bubble from outside.

#### IV. 4D TO 4D VACUUM TRANSITIONS

##### A. Geometric point of view

If we limit ourselves to ideal 4D vacua, where  $H^{-1} \gg R$ , we have

$$\frac{m_6^4}{R^2} = 2\Lambda_6 \left(1 - \frac{9H^2 m_6^4}{2\Lambda_6}\right), \quad (13)$$

$$\frac{Q^2}{m_6^8} = \frac{1}{\Lambda_6} \left(1 + \frac{3H^2 m_6^4}{\Lambda_6}\right). \quad (14)$$

Note that for these vacua,  $R \sim (m_6^4/2\Lambda_6)^{1/2}$  cannot change a lot. This gives us a few advantages. First of all, larger  $H$  in our 6D point of view really means a larger effective 4-dimensional cosmological constant. Equation (12) tells us larger  $Q$  should be outside, which agrees with the usual tunneling picture that a bigger cosmological constant should be outside. There will be geometries with a clean separation of scales,

$$R^{-1} \gg \bar{A}^{-1} \gg H_2 > H_1, \quad (15)$$

which represent standard thin-wall, small bubbles [16] that do not care for the extra dimensions. Within these solutions, we can simplify further calculations with

$$\dot{A}_1 = -\dot{A}_2 = 1 + O(H_i^2 \bar{A}^2). \quad (16)$$

Combine the junction condition Eq. (10) and (12), we have

$$\frac{\sigma}{4\pi \bar{B}^2 m_6^4} = \frac{m_6^8 \bar{A} (H_2^2 - H_1^2)}{4\Lambda_6^2 \bar{B}^4}. \quad (17)$$

Furthermore, if  $B$  does not change a lot during the transition, we have  $\bar{B} \sim R_i \sim R = (m_6^4/2\Lambda_6)^{1/2}$ . The entire transition can be understood from the 4D point of view. Using the standard dimensional reduction method, we rescale length and Planck mass as following:

$$l_{4D} = l_{6D} R m_6, \quad m_4 = \sqrt{4\pi} m_6.$$

Equation (17) reproduces the naïve junction condition in 4D,

$$\sigma_{4D} = \frac{r_c \Delta \Lambda_{4D}}{3}, \quad (18)$$

where  $r_c$  is the 4D critical size of the bubble, as expected.

##### B. Effective 4D theory

From the very beginning, we could have followed [4] and use the standard dimensional reduced effective 4D theory.

$$\begin{aligned} \sqrt{4\pi} m_6 &= m_4, & m_6 B(\rho) &= e^{(\phi(\tau))/(2m_4)}, \\ m_6 A(\rho) B(\rho) &= a(\tau), & m_6 B(\rho) d\rho &= d\tau. \end{aligned}$$

This translates the 6D Einstein equations into the general 4D Friedmann-Robertson-Walker equations and an equation of motion for the field  $\phi$ .

$$\phi'' + 3 \frac{a'}{a} \phi' = \frac{\partial V}{\partial \phi}, \quad (19)$$

$$\left(\frac{a'}{a}\right)^2 = \frac{1}{3m_4^2} \left(\frac{\phi'^2}{2} - V\right) + \frac{1}{a^2}, \quad (20)$$

$$\frac{a''}{a} = -\frac{1}{3m_4^2} (\phi'^2 + V). \quad (21)$$

Here  $'$  means the derivative to  $\tau$  and the effective potential

$$V(\phi) = m_4^2 \left( \frac{\Lambda_6}{m_6^4} e^{-(\phi/m_4)} - m_6^2 e^{-2(\phi/m_4)} + \frac{Q^2}{4} e^{-3(\phi/m_4)} \right). \quad (22)$$

In Fig. 3 we sketch the shape of effective potentials with different values of  $Q$  and indeed find a local minimum as a stable 4D vacuum. Unfortunately, different 4D vacua are present in different effective potentials, but the conventional way to describe a transition only applies to two vacua in the same potential.

However, the 6D description provides a simple answer. As depicted in Figs. 4 and 5, the field  $\phi$  follows the potential with  $Q_1$  from its vacuum value until the position of the charged brane,  $\bar{\phi} = 2m_4 \ln(m_6 \bar{B})$ , then jumps to the other potential with  $Q_2$  and proceeds to the other vacuum.

The velocity  $\bar{\phi}'$  will be discontinuous at the jump, but can be computed from the extra junction condition in 6D, Eq. (10).

$$\bar{\phi}'_1 + \bar{\phi}'_2 = \frac{3\sigma}{\sqrt{4\pi} m_6^4 \bar{B}^3}. \quad (23)$$

Since the vacuum values of  $\phi_i$  sit near each other, there will be a range of  $\phi$  where the following expansion holds in both potentials.

$$V_i(\phi) = \frac{12\pi H_i^2}{R_i^2} + \frac{2\Lambda_6^2}{m_6^{10}} (\phi - \phi_i)^2. \quad (24)$$

Here  $e^{\phi_i/2m_4} = m_6 R_i$  is the vacuum value of the field.

We can see the mass of the potential is set by the 6D vacuum energy, which is much larger than the 4D vacuum energy that controls the bounce geometry. By the argument of Coleman and De Luccia [16], we can ignore the friction

term in Eq. (19) and pretend the energy is conserved. Together with the convention we mentioned earlier, that  $\phi'$  is positive if it is increasing toward the brane, we have

$$\phi'_i = \frac{2\Lambda_6}{m_6^5}(\bar{\phi} - \phi_i), \quad (25)$$

where  $e^{\bar{\phi}/2m_4} = m_6\bar{B}$  is the matching value of the field. Plugging into the junction condition Eq. (23), we have

$$\bar{\phi} - \frac{\phi_1 + \phi_2}{2} = \frac{3\sigma m_6}{4\sqrt{4\pi\bar{B}^3\Lambda_6}}. \quad (26)$$

It is more illuminating to take the exponential of the above equation.

$$\frac{\bar{B}^2}{R_1 R_2} = e^{(3\sigma m_6)/(4\sqrt{4\pi m_4 \bar{B}^3 \Lambda_6})}. \quad (27)$$

The matching radius  $\bar{B}$  has to be larger than the geometric mean of the vacua radii for the tension to be positive. Also, depending on the tension, the transition can be monotonic as depicted in Fig. 4, or with  $\bar{B} > R_2$ , in which the field goes to a larger value then comes back, as in Figs. 6 and 7, the extra dimensions are stretched. The critical tension when  $\bar{B} = R_2$  is related to the charge  $\Delta Q$  by Eqs. (13), (27), and (14).

$$\sigma_c = 2\sqrt{2\pi m_6^2 \Delta Q}. \quad (28)$$

## V. 4D TO 6D SOLUTION

Since the extra dimensions can be stretched during a transition, more dramatic effects like decompactifications might also happen. We can use the same technique of jumping between potentials, but this time from a potential with  $Q > 0$  to  $Q = 0$ . Note that this is not covered in [5] where the entire solution is on one effective potential. The most obvious difference is the charged brane appearing explicitly in our solution.

From Eq. (12) we know that the 4D vacuum has to be outside, since it has the larger  $Q$ . It means that the non-trivial region in 4D is only a small bubble, therefore there is no major difference between a de Sitter, Minkowski or AdS space. We shall take the 4D side to be Minkowski space for simplicity. The 6D side has two possibilities. Taking the left portion in Fig. 2 we get Fig. 8, while the right portion gives Fig. 9.

Figure 8 speaks trouble. It contains a piece of de Sitter future infinity surrounded by flat spacelike asymptotics. By the argument of Farhi and Guth in [17], it needs to violate the null energy condition. In the Appendix we confirm this by showing explicitly that the junction conditions lead to a domain wall with negative tension.

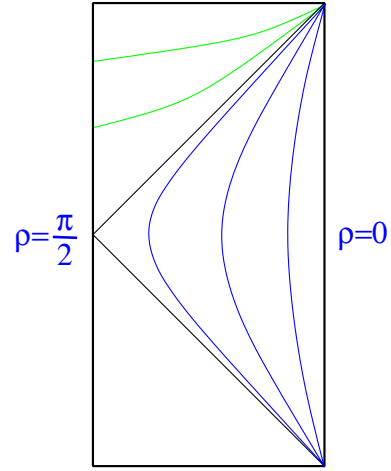


FIG. 2 (color online). The special Penrose diagram for  $dS_6$  where two  $S_2$ s are suppressed individually. One of them has zero size on the left boundary, and the other one is zero on the right boundary. Our coordinate covers the region with blue (timelike) slices where the physical radius of one  $S_2$ ,  $B(\rho)$ , is constant, and the radius of  $dS_3$  formed by the other  $S_2$  with time,  $A(\rho)$ , is also constant. These are the slicings convenient to put the charged brane. The green slices are the similar constant size surfaces with  $B > L$ , which can be obtained by analytically continuing our coordinate.

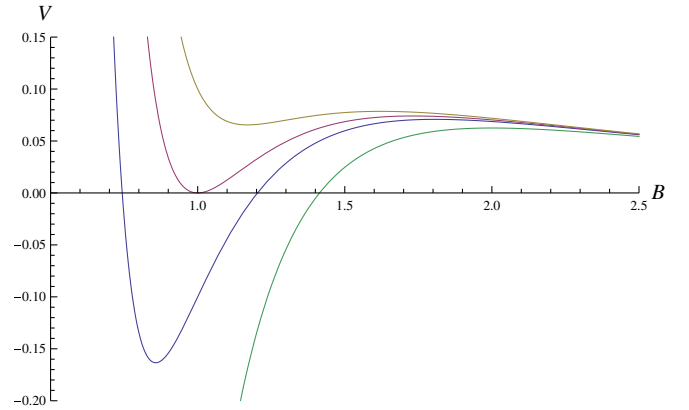


FIG. 3 (color online). Effective potential as a function of  $B = m_6^{-1}e^{\phi/(2m_4)}$ . From high to low we have potentials with decreasing  $Q$ , the stabilized 4D vacuum being de Sitter, Minkowski and AdS. The lowest one with  $Q = 0$  has no stabilized 4D vacuum.

This leaves us with Fig. 9, where the 6D piece is small and does not have de Sitter asymptotics. It is just a piece of spacetime letting the extradimensional  $S_2$  pinch off in a nonsingular way. In the Appendix we also show by junction conditions that such geometry really exists. Instead of a decompactification, we get a bubble of nothing [9]<sup>3</sup>

<sup>3</sup>We thank Ben Freivogel for pointing this out.

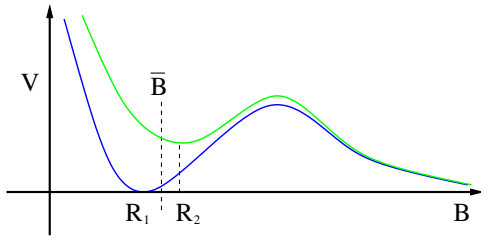


FIG. 4 (color online). The effective potential of two solutions with different charges,  $Q_1$  (blue, lower) and  $Q_2$  (green, higher). Our solution corresponds to the radius  $B$  started at  $R_2$ , moves through the green (higher) potential to  $\bar{B}$  and hits a charged brane, then follows the blue (lower) potential to  $R_1$ .

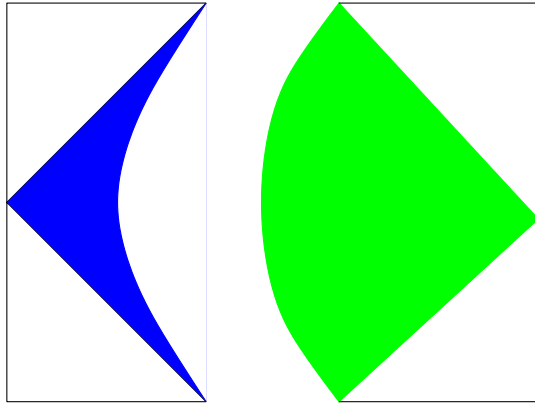


FIG. 5 (color online). The corresponding bounce geometry. The charged brane sits on the matching slice of two portions. In the left portion the field  $\phi$  follows the blue potential, and in the right portion it follows the green potential. Our metric describes the shaded parts and can be analytically continued to obtain the rest of the geometry.

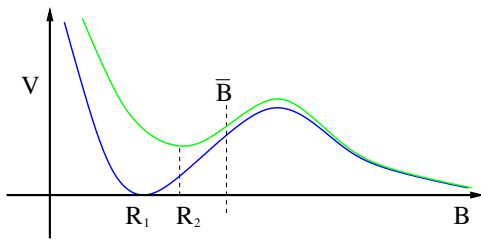


FIG. 6 (color online). The matching radius  $\bar{B}$  can be larger than either vacuum values  $R_i$ .

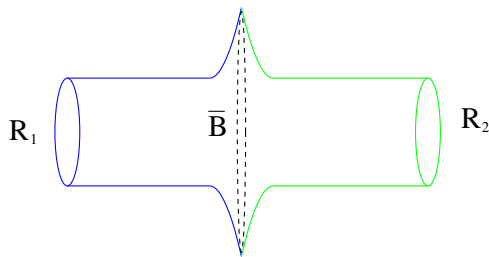


FIG. 7 (color online). The size of extra dimension  $S_2$  gets stretched during the transition from vacuum 2 (green, right) to vacuum 1 (blue, left).

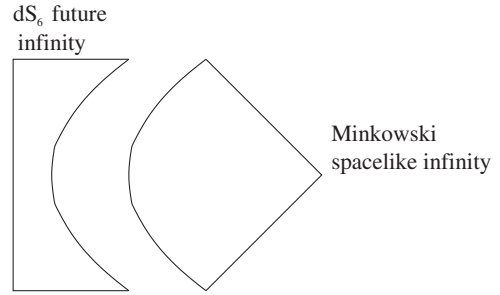


FIG. 8. Matching the interior of a small bubble in 4D Minkowski space to the bigger portion of  $dS_6$  (left-hand side of Fig. 2). Coexistence of Minkowski spacelike infinity and  $dS_6$  future infinity violates the null energy condition.

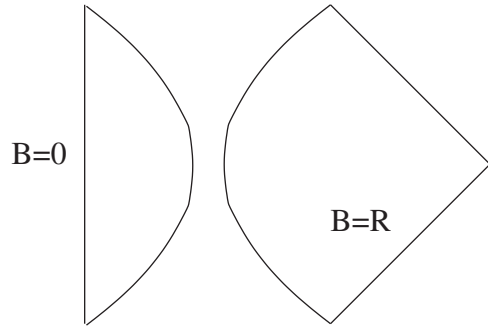


FIG. 9. Matching the interior of a small bubble in 4D Minkowski space to the smaller portion of  $dS_6$  (right-hand side of Fig. 2). The extra dimension  $S_2$  pinches off smoothly at the left end of this diagram.

## VI. DISCUSSION

### A. Stretched extra dimensions

In Sec. IV B we demonstrated a vacuum transition with extra dimensions stretched,  $(\bar{B} - R_i) \gg (R_2 - R_1)$ , in the sense that it seems to get larger than necessary while interpolating between the vacuum values. Within the validity range of our approximations, the sizes of the extra dimensions are still quite similar,  $(\bar{B} - R_i) \ll R_i$ . It means that we can still understand the geometry in the 4D picture. Also, the stretching process has the time scale of 6D physics, so from the 4D prospective it is very fast, therefore still a thin-wall solution. We did not calculate the tunneling rate explicitly because it will not be significantly different from the pure 4D Coleman–De Luccia [16] tunneling.

If we can go beyond the approximation in Eq. (25), we can increase  $\sigma$  even further and describe vacuum transitions with  $\bar{B} \gg R_i$ . In which case it will be interesting to think about the tunneling rates and many other things. In particular, there might be  $\sigma$  too large that a transition is forbidden as conjectured in [7].

A small stretch described here can already affect one thing—the bubble collisions. An interesting conjecture in [4] says that the domain walls will pass through each other

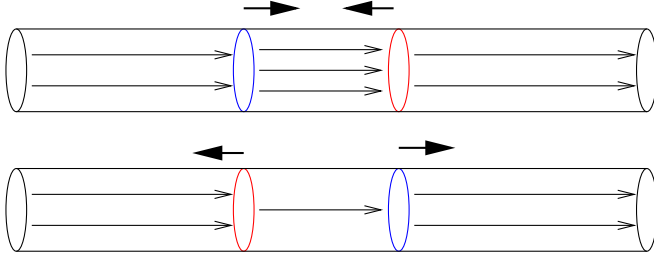


FIG. 10 (color online). Bubble collision when the extra dimensions are unstretched. If the charged branes pass through each other trivially, they will change the flux in the middle region and generate a third (lower) vacuum. With extra dimensions stretched, the charged branes will feel an additional interaction while approaching each other.

and leave a third vacuum in between, as shown in Fig. 10. It is supported by simulations of single-field-tunnelings [10]. The stretch we discovered in this paper unavoidably introduces an additional short-range interaction between domain walls. In slightly stretched or unstretched cases, the conclusion remain unchanged. However if we tune parameters to stretch the extra dimensions significantly, novel behaviors such as a collision-induced decompactification might be possible.

The critical tension to stretch the extra dimensions in Eq. (28) looks very similar to the familiar Bogomol’nyi-Prasad-Sommerfield bound in supersymmetric theories. One may want to argue that for the real string theory landscape, since we started from a supersymmetric theory, the generic object will be much heavier than the bound, and therefore always stretches the extra dimensions.

On the other hand, this toy model has 6D vacuum energy to start with. One can also argue that gravity has to be the weakest force [18].<sup>4</sup> And there must be a charged brane that does not stretch the extra dimensions.

We will not argue in favor of either side, but simply present this model as a tool to analyze the situation when the extra dimensions are stretched. For the reasons given in the Introduction, this might be an unavoidable situation.

### B. Bubbles of nothing

In Sec. V and the Appendix we provided two pieces of evidence that a bubble of nothing appears in the same way as a usual vacuum transition—through nucleation of charged branes. The Farhi-Guth [17] argument applies to the specific case in Fig. 8, where inside the bubble is a de Sitter space and outside is Minkowski. We can also adopt their argument that a small bubble effect does not care about asymptotics, therefore  $dS_4$  and  $AdS_4$  can also nucleate bubbles of nothing.

We should think about another case where we cannot apply the Farhi-Guth argument—when the higher dimen-

sional geometry is not de Sitter, but flat as in the string theory. It will be very interesting if the junction conditions still work in a similar way as in the Appendix, showing that positive tension demands a bubble of nothing instead of a decompactification.

We need to further study the decay rates. But from the fact that we can arrange our solution to be a small bubble, it should have a rate very similar to a standard thin-wall quantum instanton [4,16,19]. Other geometries representing decompactification tunnelings all have rates close to a thermal instanton [4,5,8,11]. This may suggest that bubbles of nothing is the real universal instability we should think about, not decompactifications.

### ACKNOWLEDGMENTS

We thank Ben Freivogel for numerous discussions and interesting suggestions that helped to shape this paper. We also thank Raphael Bousso, Matthew Johnson and Robert Myers for stimulating discussions. This work is supported in part by the U.S. Department of Energy, and partially done in the Berkeley Center of Theoretical Physics.

### APPENDIX: A CASE STUDY FOR 4D TO 6D TRANSITIONS

Here we will construct a specific example of bubble of nothing geometry—part of which is exactly a piece of  $dS_6$ —to support the argument and claim in Sec. V that such geometry exists in the flux compactification scenario. We believe the more general geometry also exists but it is beyond the scope of this paper.

In Sec. IV we followed a general process to find the matching geometry with given  $Q_1$ ,  $Q_2$ ,  $\Lambda_6$  and  $\sigma$ , which relies heavily on the approximation in Eq. (25), and the fact that on either side we can find a family of well-behaved solutions all similar to the 4D stabilized geometry.

Unfortunately, Eq. (25) does not hold anywhere on the  $Q = 0$  potential, and even the naïve  $dS_6$  solution in Eq. (4) looks dangerously singular in the 4D equations of motion (19). A very careful numerical study might solve the problem, but we would like to do something slightly different here.

Instead of searching for geometries with all parameters fixed, we would like to specify the geometry at the  $Q = 0$  side. As a trade-off, the tension  $\sigma$  cannot be fixed anymore. We will show that in order to get the geometry in Fig. 8, the tension has to be negative. This agrees with our reasoning in Sec. V that it violates the null energy condition. For the geometry in Fig. 9, the solution works with a positive tension.

The  $Q = 0$  geometry will be specified as the pure  $dS_6$  solution in Eq. (4). With the convention that  $\rho$  increases as it approaches the junction, it is like Fig. 9.

$$A_1(\rho) = L \cos \frac{\rho}{L}, \quad B_1(\rho) = L \sin \frac{\rho}{L}. \quad (A1)$$

<sup>4</sup>We thank Robert Myers for pointing this out.

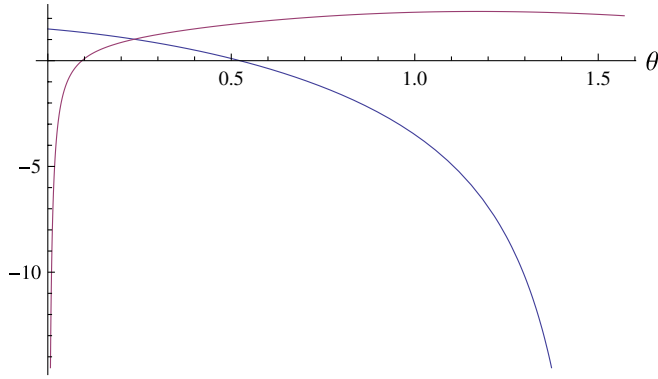


FIG. 11 (color online). The two junction conditions for the bubble of nothing geometry. They cross at a positive  $\sigma$ .

For Fig. 8, we only need to exchange  $A$  and  $B$ .

$$A_1(\rho) = L \sin \frac{\rho}{L}, \quad B_1(\rho) = L \cos \frac{\rho}{L}. \quad (\text{A2})$$

From the junction conditions, Eq. (10), we have

$$\dot{A}_2 = -\frac{\bar{A}\sigma}{16\pi\bar{B}^2 m_6^4} - \dot{A}_1, \quad (\text{A3})$$

$$\dot{B}_2 = \frac{3\bar{B}\sigma}{16\pi\bar{B}^2 m_6^4} - \dot{B}_1. \quad (\text{A4})$$

By Eq. (14),  $Q_2 = m_6^4/\sqrt{\Lambda_6}$  has the 4D Minkowski vacuum. The effective potential is

$$V(\bar{B}) = \frac{2\pi}{R^2\bar{B}^2} \left(1 - \frac{R^2}{\bar{B}^2}\right)^2. \quad (\text{A5})$$

For this potential we can still use the same approximation in Eq. (25).

$$\phi' = \frac{2\sqrt{\pi}}{R\bar{B}} \left(1 - \frac{R^2}{\bar{B}^2}\right). \quad (\text{A6})$$

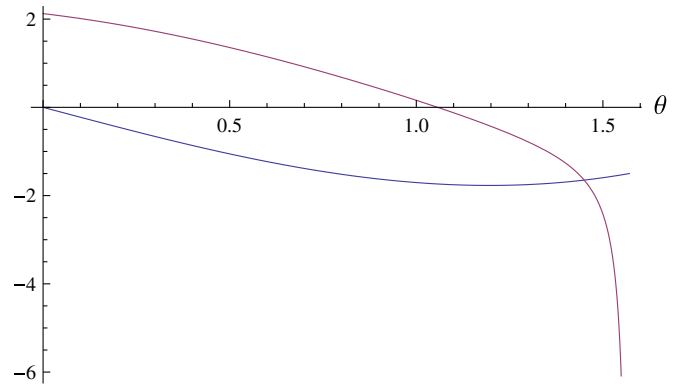


FIG. 12 (color online). The two junction conditions for the decompactification geometry. They cross at a negative  $\sigma$ .

Relate  $\phi'$  to  $\dot{B}_2$  and use Eq. (A4), we have

$$\dot{B}_1 + \frac{\bar{B}}{2R} \left(1 - \frac{R^2}{\bar{B}^2}\right) = \frac{3\sigma}{16\pi\bar{B}m_6^4}. \quad (\text{A7})$$

As a small bubble in 4D Minkowski space,

$$\bar{A} \frac{\dot{B}_2}{\bar{B}} + \dot{A}_2 = a' = -1. \quad (\text{A8})$$

Combine with Eqs. (A3) and (A4), we have

$$\frac{3\bar{B}}{2\bar{A}} \left(\dot{A}_1 + \frac{\bar{A}}{\bar{B}} \dot{B}_1 - 1\right) = \frac{3\sigma}{16\pi\bar{B}m_6^4}. \quad (\text{A9})$$

Note that Eqs. (A7) and (A9) have the same right-hand side. Also, since  $L = \sqrt{10}m_6^2/\sqrt{\Lambda_6} = 2\sqrt{5}R$ , the left-hand sides are just sin and cos. Plotting them between 0 and  $\pi/2$ , we found that with Eq. (A1) they cross at a positive  $\sigma$  (as in Fig. 11), but with Eq. (A2) they cross at a negative  $\sigma$  (as in Fig. 12). This confirms the argument in Sec. V that Fig. 8 violates the null energy condition, and the bubble of nothing geometry in Fig. 9 really exists.

- 
- [1] P.G.O. Freund and M.A. Rubin, *Phys. Lett. B* **97**, 233 (1980).  
[2] S. Randjbar-Daemi, A. Salam, and J.A. Strathdee, *Nucl. Phys.* **B214**, 491 (1983).  
[3] M.R. Douglas and S. Kachru, *Rev. Mod. Phys.* **79**, 733 (2007).  
[4] J.J. Blanco-Pillado, D. Schwartz-Perlov, and A. Vilenkin, *J. Cosmol. Astropart. Phys.* **12** (2009) 006.  
[5] S.M. Carroll, M.C. Johnson, and L. Randall, *J. High Energy Phys.* **11** (2009) 094.  
[6] R. Bousso and J. Polchinski, *J. High Energy Phys.* **06** (2000) 006.  
[7] M.C. Johnson and M. Larfors, *Phys. Rev. D* **78**, 123513 (2008).  
[8] S.B. Giddings and R.C. Myers, *Phys. Rev. D* **70**, 046005 (2004).  
[9] E. Witten, *Nucl. Phys.* **B195**, 481 (1982).  
[10] R. Easther, J. Giblin, T. John, L. Hui, and E.A. Lim, *Phys. Rev. D* **80**, 123519 (2009).  
[11] S. Kachru, R. Kallosh, A. Linde, and S.P. Trivedi, *Phys. Rev. D* **68**, 046005 (2003).  
[12] J.J. Blanco-Pillado *et al.*, *J. High Energy Phys.* **11** (2004) 063.  
[13] R. Bousso, O. DeWolfe, and R.C. Myers, *Found. Phys.* **33**, 297 (2003).  
[14] C. Krishnan, S. Paban, and M. Zanic, *J. High Energy Phys.*

- 05 (2005) 045.
- [15] W. Israel, *Nuovo Cimento B* **44S10**, 1 (1966).
- [16] S. Coleman and F. De Luccia, *Phys. Rev. D* **21**, 3305 (1980).
- [17] E. Farhi and A. H. Guth, *Phys. Lett. B* **183**, 149 (1987).
- [18] N. Arkani-Hamed, L. Motl, A. Nicolis, and C. Vafa, *J. High Energy Phys.* **06** (2007) 060.
- [19] A. R. Brown and E. J. Weinberg, *Phys. Rev. D* **76**, 064003 (2007).